Competing Orders in FeAs Layers

J. Lorenzana,[1,2] G. Seibold,[3] C. Ortix,[4] and M. Grilli[1]

[1]*SMC-INFM-CNR and Dipartimento di Fisica, Università di Roma "La Sapienza," Piazzale Aldo Moro 2, 00185 Roma, Italy*
[2]*ISC-CNR, Via dei Taurini 19, 00185 Roma, Italy*
[3]*Institut für Physik, BTU Cottbus, PBox 101344, 03013 Cottbus, Germany*
[4]*Institute Lorentz for Theoretical Physics, Leiden University, P.O. Box 9506, 2300 RA Leiden, The Netherlands*
(Received 28 July 2008; published 29 October 2008)

Using the unrestricted Hartree-Fock approximation and Landau theory we identify possible phases competing with superconductivity in FeAs layers. We find that close to half-filling the transition from the paramagnet to the magnetically ordered phase is first order, making anharmonicities relevant and leading to a rich phase diagram. Between the already known one-dimensionally modulated magnetic stripe phase and the paramagnet we find a new phase which has the same structure factor as the former but in which magnetic moments at nearest-neighbor sites are at right angles making electrons acquire a nontrivial phase when circulating a plaquette at strong coupling. Another competing phase has magnetic and charge order and may be stabilized by charged impurities.

Exotic superconductivity often appears in a phase diagram region where a uniform paramagnetic (PM) phase competes with charge or magnetic order. Examples are the heavy fermion compounds [1], organics [2], vanadium bronzes [3], transition-metal chalcogens [4], and barium bismuthates [5,6]. A competing phase is believed to play an important role in Cu-based high temperature superconductors probably with charge and magnetic order [7]. One important question is if the competing phase is only detrimental for superconductivity [8] or if its vicinity helps superconductivity [9–12].

In the recently discovered Fe-based superconductors [13–15], the Coulomb interaction is believed to be relatively weaker than in cuprates making a mean-field analysis more likely to lead to a quick identification of the possible competing phases. Indeed first-principles computations [16] have predicted a magnetic stripe (MS) phase with ordering wave vector $(\pi, 0)$ (we define wave vectors for an isolated FeAs layer with the primitive vectors connecting nearest Fe sites and Fe-Fe distance $a \equiv 1$) which later has been found by magnetic neutron scattering in two different families of compounds [17,18].

Here we extend the analysis using the unrestricted Hartree-Fock (HF) approximation in a model Hamiltonian which keeps only two orbitals supplemented with a Landau theory analysis. This allows more flexibility than first-principles computations to identify possible competing phases at the expense of more (yet) unknown parameters. Surprisingly, we find a new magnetic phase in which magnetic moments at nearest neighbor sites are at right angles which we term orthomagnetic (OM). This is interesting in its own because well-formed magnetic moments usually lead to phases in which magnetic moments are either mutually parallel or antiparallel [19,20]. We identify another competing phase which has both spin and charge order (SCO) reminiscent to the stripe phases of

cuprates. This phase may be locally stabilized by charged impurities.

Our starting point is the two-orbital Hamiltonian $H = H_0 + H_{\text{int}}$ [21–24] with the noninteracting part (here written in momentum space)

$$H_0 = \sum_{\mathbf{k}\alpha\sigma} \varepsilon_\alpha(\mathbf{k}) d^\dagger_{\mathbf{k}\alpha\sigma} d_{\mathbf{k}\alpha\sigma}$$
$$+ \sum_{\mathbf{k}\sigma} \varepsilon_{xy}(\mathbf{k})(d^\dagger_{\mathbf{k}x\sigma} d_{\mathbf{k}y\sigma} + d^\dagger_{\mathbf{k}y\sigma} d_{\mathbf{k}x\sigma}),$$

$$\varepsilon_x(\mathbf{k}) = -2t_1 \cos(k_x) - 2t_2 \cos(k_y) - 4t_3 \cos(k_x)\cos(k_y),$$

$$\varepsilon_y(\mathbf{k}) = -2t_2 \cos(k_x) - 2t_1 \cos(k_y) - 4t_3 \cos(k_x)\cos(k_y),$$

$$\varepsilon_{xy}(\mathbf{k}) = -4t_4 \sin(k_x)\sin(k_y) \tag{1}$$

where $d^\dagger_{\mathbf{k}\alpha\sigma}$ creates an electron in orbital $d_{\alpha z}$ in momentum space with $\alpha = x, y$. The interaction part includes an intra- and interorbital repulsion and a Hund coupling term (here defined in real space):

$$H_{\text{int}} = U \sum_{i\alpha} n_{i\alpha\uparrow} n_{i\alpha\downarrow} + U' \sum_i n_{ix} n_{iy} - 2J \sum_i \mathbf{S}_{ix} \cdot \mathbf{S}_{iy}$$

with $n_{i\alpha\sigma}$ the occupation operator for orbital α with spin σ, $n_{i\alpha} \equiv n_{i\alpha\uparrow} + n_{i\alpha\downarrow}$, and $\mathbf{S}_{i\alpha}$ the spin operator. We neglect the small spin-orbit coupling [25] so the Hamiltonian is rotationally invariant in spin space. We also considered a pair hopping term and found that does not affect our mean-field results [24]. In the following we adopt the hopping parameters from Ref. [24] and we define the intraorbital repulsion by the standard relation $U' = U - 3J/2$ and $J = 0.25U$ for definiteness.

Phases were identified using a fully unrestricted HF approximation in large clusters (typically 14×14) with periodic boundary conditions. Subsequently the energy of each solution has been computed in much larger systems treated in momentum space. In the latter case we neglected

a small canting of the MS solution which has a negligible effect on the energy.

In the upper panel of Fig. 1 we show the resulting phase diagram of the two-orbital model in the U-density plane at zero temperature. The solid circle is a tricritical point: to the left of it the transition is weakly first order whereas to the right it is second order. Between the MS and the PM we find the new OM phase in which magnetic moments at nearest-neighbor sites are at right angles as shown in the inset of the upper panel of Fig. 1. It can be seen as the superposition of two magnetic stripes perpendicular to each other. The magnetization at position $\mathbf{R}_l$ reads

$$\mathbf{m}_l = \sum_{i=1}^{2} \mathbf{M}_i \exp(i\mathbf{Q}_i \cdot \mathbf{R}_l) \qquad (2)$$

with $\mathbf{Q}_1 \equiv (0, \pi)$, $\mathbf{Q}_2 \equiv (\pi, 0)$ and $\mathbf{M}_1$, $\mathbf{M}_2$ mutually perpendicular and equal in modulus. The MS is recovered by setting one of the $\mathbf{M}_i$ in Eq. (2) to zero.

The first-order character of the transition close to half-filling is not surprising given that the model is quite frustrated from the magnetic point of view [26]. Increasing U the system can avoid frustration by staying in the PM phase until the point in which the energy penalty of not forming magnetic moments becomes too large driving the system through the abrupt transition to a magnetic phase.

We find the topology of the phase diagram shown in Fig. 1 to be rather robust, although for some parameters [23] the tricritical point becomes a triple point. Even more, we find essentially the same topology in a standard one-

band Hubbard model supplemented with an explicit anti-ferromagnetic next-nearest-neighbor magnetic interaction J' across the diagonals. The latter frustrates the usual Néel state and favors the magnetic instability at $\mathbf{Q}_i$.

The larger stability of the OM phase compared to the MS at half-filling is due to the fact that this two-dimensional texture opens gaps in the electronic structure in both x and y directions whereas the MS in weak coupling leaves the direction parallel to the stripes metallic. Therefore a more stable fully gaped (insulating) solution is found for a weaker coupling in the OM case than in the MS case. This is illustrated in the lower panels of Fig. 1 where we show the density of states (DOS) for both solutions and $U = 0.8$ eV. For smaller U both solutions are metallic but the OM state has a deeper pseudogap.

The dips in the OM DOS close to 1/4 filling and 3/4 filling can be understood in strong coupling as due to the fact that as an electron from the lower (upper) Hubbard band circulates a plaquette, the HF potential forces its spin to be parallel (antiparallel) to the local direction of the magnetization. Thus after a complete loop the electron spin gets back to the original direction but the single particle wave function acquires a phase $e^{i\pi} = -1$ reminiscent of the staggered flux phase in cuprates [27,28]. This produces a conelike dispersion and a semimetallic DOS which evolves into the dips in weak coupling.

More insight on the phase diagram can be obtained with the following Landau toy model in terms of the Fourier transform of the magnetization:

$$
\begin{aligned}
\delta f = {} & \frac{1}{2}\sum_{\mathbf{q}} \chi^{-1}(\mathbf{q})\mathbf{m}_{\mathbf{q}} \cdot \mathbf{m}_{-\mathbf{q}} \\
& + \beta_1 \sum_{\mathbf{q}_1 \dots \mathbf{q}_4} (\mathbf{m}_{\mathbf{q}_1} \cdot \mathbf{m}_{\mathbf{q}_2})(\mathbf{m}_{\mathbf{q}_3} \cdot \mathbf{m}_{\mathbf{q}_4})\delta_{\mathbf{q}_1+\mathbf{q}_2+\mathbf{q}_3+\mathbf{q}_4,0} \\
& + \gamma_1 \sum_{\mathbf{q}_1 \dots \mathbf{q}_6} (\mathbf{m}_{\mathbf{q}_1} \cdot \mathbf{m}_{\mathbf{q}_2})(\mathbf{m}_{\mathbf{q}_3} \cdot \mathbf{m}_{\mathbf{q}_4})(\mathbf{m}_{\mathbf{q}_5} \cdot \mathbf{m}_{\mathbf{q}_6}) \\
& \times \delta_{\mathbf{q}_1+\mathbf{q}_2+\mathbf{q}_3+\mathbf{q}_4+\mathbf{q}_5+\mathbf{q}_6,0}. \qquad (3)
\end{aligned}
$$

It consists of a Gaussian part and a local interaction part which we keep up to sixth order to be able to describe both second- and first-order phase transitions. We assume that the susceptibility $\chi(\mathbf{q})$ diverges, for a set of symmetry related momenta $\mathbf{Q}_i$, at an instability line controlled by the parameter $\alpha \equiv \chi^{-1}(\mathbf{Q}_i)$ and take $\gamma_1 > 0$ for stability. The non-Gaussian vertices have been taken as momentum independent in the same spirit of Ref. [29]. This will be partially relaxed below.

For $\beta_1 > 0$ the above model describes an ordinary second-order magnetic phase transition as α crosses the Gaussian line $\alpha = 0$. For $\beta_1 < 0$ there is a first-order phase transition with a tricritical point at $(\beta_1, \alpha) = (0, 0)$. This can be treated analogously to the liquid-solid transition [30] and frustrated phase separation [31]. Crucially, the non-Gaussian terms may favor magnetic textures build by the superposition of several harmonics. As in Refs. [30,31],
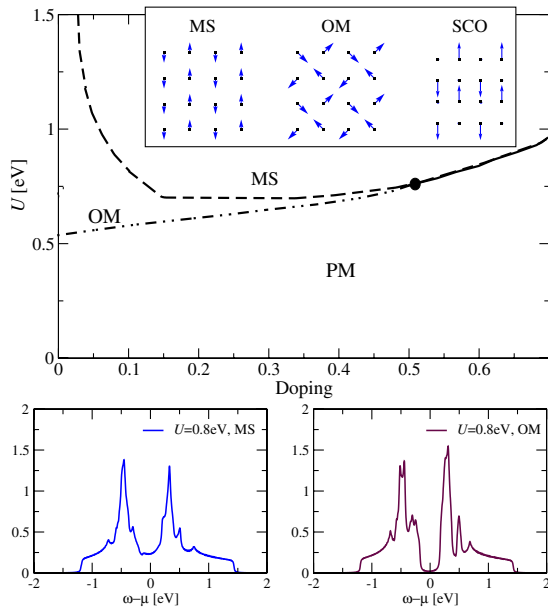

FIG. 1 (color online). Upper panel: $T = 0$ phase diagram of the two-orbital model in the U-density plane. The solid circle is the tricritical point. The insets shows the magnetic structure of the ordered phases considered in this study. Lower panels: The local HF DOS for the MS and OM states.

to minimize the energy we restrict the sums in Eq. (3) to the $\mathbf{Q}_i$ set. The magnetic texture is formed by subsets which satisfy the Kronecker delta of the quartic term modulo a reciprocal lattice vector. Only two choices are possible: either all the $\mathbf{q}_i$ are the same and equal to one $\mathbf{Q}_i$ which leads to the MS or the $\mathbf{q}_i$ are equal in pairs to one of the $\mathbf{Q}_i$. In the latter case we still have to choose the relative angle between the two vectorial Fourier components $\mathbf{M}_i$ at $\mathbf{Q}_i$ [c.f. Eq. (2)] and their magnitudes, M_i [32]. For two-dimensional textures we find that the energy is locally minimized when the magnitude of the two amplitudes is the same and the angle between the two Fourier components is either $\pi/2$ (which leads to the OM state) or zero. The latter is a new phase in which the real space magnetization is zero in one sublattice and forms an antiferromagnetic structure in the other sublattice. This is the only phase we have found in which the modulus of the magnetization is not uniform (labeled SCO in the inset of Fig. 1). Since the charge density is a scalar, it couples with the square of the magnetization. It follows that this phase will have SCO reminiscent of the charged stripe phases in cuprates [7]. In the present case the charge ordering wave vector is (π, π). In the following, for simplicity, we neglect the effect of the charge relaxation upon the energy, which in any case does not affect the quadratic terms. Indeed we find in HF that this effect is small.

Calling M_T the magnitude of the magnetization in real space, we find that the MS and the OM phase have the same energy [33] given by $\delta f_{\mathrm{OM,MS}} = \alpha M_T^2/2 + \beta_1 M_T^4 + \gamma_1 M_T^6$ while for the SCO phase $\delta f_{\mathrm{SCO}} = \delta f_{\mathrm{OM,MS}}/2$. These energies are easily rationalized from the fact that the non-Gaussian terms in Eq. (3) are local in real space and in the SCO state only half of the sites are magnetized (c.f. inset in Fig. 1).

The phase diagram is shown in Fig. 2(a). The dashed line is the limit of metastability of the magnetic phases. The insets show the behavior of f in the metastable regions. The $1/2$ factor in the energy makes the MS and OM configurations more stable than the SCO configurations in the ordered region. As soon as the phase boundary is crossed and one reaches the PM phase the situation is reversed. The lowest energy phase above the PM is the "hidden" SCO phase. Proximity of the paramagnet to this phase is suggestive in view that the charge ordering is similar to the one in $\mathrm{BaBiO_3}$ which becomes superconducting when doped [5,6].

In the restricted HF approximation for the parameters of Ref. [24] and positive doping we have found that the PM-SCO transition is second order; thus, the SCO phase cannot become metastable as in the Landau toy model, but of course this is sensitive to the parameter set. For other parameters [23] we have even found a region of SCO phase in the phase diagram at high doping.

The Landau toy model phase diagram is oversimplified and does not even reproduce the full physics of the HF phase diagram. One can construct a canonical Landau theory as follows. First the magnetization is written as the sum of products of slowly varying parts $\mathbf{M}_i(\mathbf{R})$ times rapidly varying parts $\exp(i\mathbf{Q}_i \cdot \mathbf{R}_l)$. The energy can be expanded close to the Gaussian line in terms of the invariants generated by the $\mathbf{M}_i(\mathbf{R})$ and its gradients. We are interested in uniform phases so we neglect the spacial dependence of the order parameters $\mathbf{M}_i$ reaching Eq. (2).

We have two second-order invariants $I_i \equiv \mathbf{M}_i \cdot \mathbf{M}_i$. The fourth-order invariants are powers of the second-order ones and $I_3 \equiv (\mathbf{M}_1 \cdot \mathbf{M}_2)^2$ and $I_4 \equiv (\mathbf{M}_1 \times \mathbf{M}_2) \cdot (\mathbf{M}_1 \times \mathbf{M}_2)$. The latter can be eliminated since it depends on the other invariants through the relation $I_3 + I_4 = I_1 I_2$.

The energy can be written as

$$\delta F = \frac{1}{2}\alpha \sum_{i=1}^{2} \mathbf{M}_i \cdot \mathbf{M}_i + \beta_1 \sum_{i=1}^{2}(\mathbf{M}_i \cdot \mathbf{M}_i)^2 + \beta_2(\mathbf{M}_1 \cdot \mathbf{M}_2)^2$$
$$+ \beta_3(\mathbf{M}_1 \cdot \mathbf{M}_1)(\mathbf{M}_2 \cdot \mathbf{M}_2) + \gamma_1 \sum_{i=1}^{2}(\mathbf{M}_i \cdot \mathbf{M}_i)^3$$
$$+ \gamma_2(\mathbf{M}_1 \cdot \mathbf{M}_2)^2 \sum_{i=1}^{2} \mathbf{M}_i \cdot \mathbf{M}_i$$
$$+ \gamma_3[(\mathbf{M}_1 \cdot \mathbf{M}_1)(\mathbf{M}_2 \cdot \mathbf{M}_2)^2 + (\mathbf{M}_1 \cdot \mathbf{M}_1)^2(\mathbf{M}_2 \cdot \mathbf{M}_2)].$$
$$(4)$$

In this case the energy of the different phases is

$$\delta f_{\mathrm{MS}} = \frac{\alpha}{2} M_T^2 + B_1 M_T^4 + G_1 M_T^6,$$
$$\delta f_{\mathrm{OM}} = \frac{\alpha}{2} M_T^2 + B_2 M_T^4 + G_2 M_T^6,$$
$$\delta f_{\mathrm{SCO}} = \frac{1}{2}\left(\frac{\alpha}{2} M_T^2 + B_3 M_T^4 + G_3 M_T^6\right),$$

with $B_1 = \beta_1$, $B_2 = (2\beta_1 + \beta_3)/4$, $B_3 = (2\beta_1 + \beta_2 + \beta_3)/8$, $G_1 = \gamma_1$, $G_2 = (\gamma_1 + \gamma_3)/4$, $G_3 = (\gamma_1 + \gamma_2 + \gamma_3)/16$.

The parameters of the model can be fixed by comparing observables with experiment. One can consider the former to be a function of two or more control parameters (like U, doping, P, and T). Taking two control parameters for simplicity, each ordered phase considered alone can have
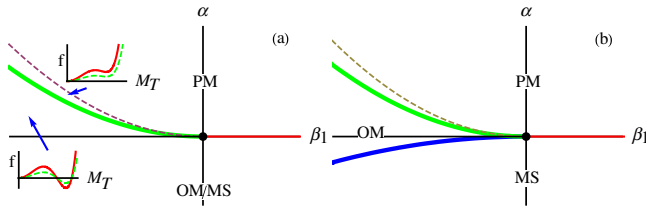

FIG. 2 (color online). Phase diagram for the Landau toy model (a) and the full Landau model (b). The dashed line is the limit of metastability of the ordered phases. The limit of metastability of the PM phase is given by the line $\alpha = 0$. The thick lines represent weakly first-order transitions ending at the tricritical point. The insets show the behavior of the energy for the magnetic phases (full line) and the SCO phase (dashed line) in the regions of metastability.

a different tricritical point with the paramagnet. If instead all phases are allowed to compete, depending on parameters one can have more complex phase diagrams including triple points. It is interesting that for temperature driven transitions both first- and second-order transitions have been observed, depending on the material [34], which suggests proximity to a tricritical point.

Given the local character of the electronic interactions, we expect the parameters to be not far from those of the Landau toy model Eq. (3), which corresponds to $B_i = \beta_1$, $G_i = \gamma_1$. Indeed one can obtain the same topology as in HF taking $B_1 = \beta_1$, $B_2 = 1.07\beta_1$, $B_3 > \max(0, \beta_1/2)$, $G_2 = 1.1\gamma_1$, and $G_1 = G_3 = \gamma_1$ [c.f. Fig. 2(b)].

The four phases identified (PM, OM, MS, SCO) are the only phases allowed by the model Eq. (4); thus, our study is exhaustive close to the Gaussian line (which for the first-order region means close to the tricritical point). The exceptions are special combinations of parameters where a family of solutions become degenerate as in the Landau toy model [33]. Canting of the magnetic moments respect to the identified solutions require higher order terms in the Landau free energy.

It is easy to check that the structure factor averaged to take into account a superposition of randomly oriented domains is the same for the OM and MS phases; thus, in principle, it can be difficult to distinguish among them with a magnetic neutron scattering experiment alone on polycrystalline samples. In practice, nuclear neutron scattering detects also a lattice distortion which breaks the C_{4v} symmetry of the lattice and most likely stabilizes the MS [17,26]. It is possible that the OM state can be stabilized suppressing the structural transition by pressure or chemical substitution.

The SCO phase may be locally stabilized by charged impurities. We expect the concomitant spin and charge order to appear around charged nonmagnetic impurities, which may be observed with local probes like NMR, nuclear quadrupole resonance, Mössbauer, and scanning tunneling spectroscopy.

In conclusion, we have exhaustively analyzed possible magnetic phases competing with superconductivity in FeAs layers close to the Gaussian instability line of the paramagnet. Because of magnetic frustration we find a tendency for PM-magnetic transitions to be first order as shown in the HF approximation. Contrary to general beliefs the two-orbital minimal model [24] does not show the MS phase close to half-filling. Instead we find a new phase in which magnetic moments acquire an unusual orthogonal configuration. We find another low energy phase with spin order and charge order at momentum (π, π) which provides an obvious link among charge fluctuations, possibly relevant for superconductivity, and magnetism. Our results provide a guide of likely configurations to be found in the phase diagram of layered FeAs based compounds and a Landau framework to study them.

[1] N. D. Mathur *et al.*, Nature (London) **394**, 39 (1998).
[2] R. H. Mckenzie, Science **278**, 820 (1997).
[3] T. Yamauchi, Y. Ueda, and N. Môri, Phys. Rev. Lett. **89**, 057002 (2002).
[4] E. Morosan *et al.*, Nature Phys. **2**, 544 (2006).
[5] L. F. Mattheiss, E. M. Gyorgy, and D. W. Johnson, Phys. Rev. B **37**, 3745 (1988).
[6] S. Pei *et al.*, Phys. Rev. B **41**, 4126 (1990).
[7] J. M. Tranquada *et al.*, Nature (London) **375**, 561 (1995).
[8] C. A. Balseiro and L. M. Falicov, Phys. Rev. B **20**, 4457 (1979).
[9] C. Castellani, C. Di Castro, and M. Grilli, Phys. Rev. Lett. **75**, 4650 (1995).
[10] S. A. Kivelson, E. Fradkin, and V. J. Emery, Nature (London) **393**, 550 (1998).
[11] A. V. Chubukov, D. Pines, and B. P. Stojkovic, J. Phys. Condens. Matter **8**, 10017 (1996).
[12] M. Capone, M. Fabrizio, C. Castellani, and E. Tosatti, Science **296**, 2364 (2002).
[13] Y. Kamihara, T. Watanabe, M. Hirano, and H. Hosono, J. Am. Chem. Soc. **130**, 3296 (2008).
[14] M. Rotter, M. Tegel, and D. Johrendt, Phys. Rev. Lett. **101**, 107006 (2008).
[15] K. Sasmal *et al.*, Phys. Rev. Lett. **101**, 107007 (2008).
[16] J. Dong *et al.*, Europhys. Lett. **83**, 27006 (2008).
[17] C. de la Cruz *et al.*, Nature (London) **453**, 899 (2008).
[18] K. Kaneko *et al.*, arXiv:0807.2608.
[19] C. Xu, M. Müller, and S. Sachdev, Phys. Rev. B **78**, 020501(R) (2008).
[20] C. Fang *et al.*, Phys. Rev. B **77**, 224509 (2008).
[21] Q. Han, Y. Chen, and Z. D. Wang, Europhys. Lett. **82**, 37007 (2008).
[22] T. Li, arXiv:0804.0536, 2008.
[23] S. Raghu *et al.*, Phys. Rev. B **77**, 220503(R) (2008).
[24] M. Daghofer *et al.*, arXiv:0805.0148.
[25] H. S. Jeevan *et al.*, Phys. Rev. B **78**, 052502 (2008).
[26] T. Yildirim, Phys. Rev. Lett. **101**, 057010 (2008).
[27] X. G. Wen and P. A. Lee, Phys. Rev. Lett. **76**, 503 (1996).
[28] I. Affleck and J. B. Marston, Phys. Rev. B **37**, 3774 (1988).
[29] J. A. Hertz, Phys. Rev. B **14**, 1165 (1976).
[30] S. Alexander and J. McTague, Phys. Rev. Lett. **41**, 702 (1978).
[31] C. Ortix, J. Lorenzana, and C. Di Castro, Phys. Rev. Lett. **100**, 246402 (2008).
[32] Notice that because of spin rotational symmetry the energy is invariant with respect to a global rotation of the magnetizations.
[33] For the Landau toy model we find that the energy of solutions with $\mathbf{M}_1$ and $\mathbf{M}_2$ orthogonal depend only on $M_T^2 \equiv M_1^2 + M_2^2$ and not on $\delta M^2 \equiv M_1^2 - M_2^2$ leading to a family of degenerate phases.
[34] C. Krellner *et al.*, Phys. Rev. B **78**, 100504(R) (2008).